

*XVII IMEKO World Congress
Metrology in the 3rd Millennium
June 22–27, 2003, Dubrovnik, Croatia*

PULSED REMOTE FIELD TECHNIQUE IN FERROMAGNETIC TUBE WALL THICKNESS AND INNER DIAMETER MEASUREMENT

*Darko Vasić, Vedran Bilas, Davorin Ambruš**

Faculty of Electrical Engineering and Computing, University of Zagreb, Zagreb, Croatia

*Brodarski Institute, Zagreb, Croatia

Abstract – In conventional applications of the remote field eddy current technique, a probe with low frequency sinusoidal excitation is used for measurement of ferromagnetic tube wall thickness. An additional probe with high frequency excitation is required for measurement of the tube inner diameter (electrical caliper). In this paper, this is illustrated with results of finite element analysis. However, the waveform of the pulse driving current and shorter probe length potentially allow the measurement of the inner diameter and the wall thickness with the same probe. We present results of our experiments on ferromagnetic tubes with internal and external defects that confirm applicability of the pulsed remote field technique for measurement of the both quantities.

Keywords: pulsed eddy current, pulsed remote field technique, wall thickness and inner diameter measurement.

1. INTRODUCTION

Remote field eddy current (RFEC) technique is a well-known and highly effective electromagnetic method for measurement of ferromagnetic tube wall thickness [1].

The basic RFEC probe consists of an exciter coil and a detector coil. The exciter coil produces a time varying magnetic field that induces eddy currents within the material (i.e. tube wall). Voltage u_d induced in the detector coil has two components: u_e induced directly by the exciter magnetic field and u_{ec} induced by the magnetic field of the eddy currents. Since the eddy currents flow through the tube wall, the component u_{ec} carries information about the wall thickness or the inner diameter depending on the distance between the coils and excitation frequency [2]. The voltage u_{ec} is influenced by the electromagnetic properties of the tube material (permeability and conductivity). Therefore, gauging in the intact part of the tube prior to the measurement in rest of the tube is required [1].

Conventional RFEC technique uses sinusoidal excitation (<100Hz) and coils separated 2-3 tube diameters. Such a large distance is required to make the component u_{ec} dominant and sensitive to the wall thickness. RFEC technique cannot differentiate whether the wall thickness is changed by an internal or an external defect (i.e. to measure the tube inner diameter). For measurement of the tube inner diameter, two additional coils spaced for around 1 tube

diameter and high frequency excitation are applied (“electrical caliper”) [4, 5].

Recently, attention has been paid to potential application of pulse instead of sinusoidal driving current. Finite element study of pulsed RFEC phenomena has suggested its potential usefulness for detection of wall defects of the ferromagnetic tubes [6]. In our previous work, we have experimentally verified its applicability for the wall thickness measurement with significant reduction of the required power [7]. However, in spite of continuous spectrum of the pulse excitation, sensitivity to the tube inner diameter has not been observed in the remote zone.

Sinusoidal excitation causes constant presence of the component u_e of the voltage u_d induced in the detector coil. In the case of pulse excitation, the component u_e exists only during the rise or fall of the excitation current. That limited duration of the voltage u_e improves sensitivity to the wall thickness measurement. Also, pulse excitation enables separation in time of responses sensitive to inner diameter and wall thickness for the same detector location [2].

In this paper we present a method for measuring both the tube wall thickness and the inner diameter with the pulse driven, considerably shorter RFEC probe consisting only of one pair of coils.

2. METHODS AND MATERIALS

2.1. Finite Element Analysis

Sensitivity of the tube wall thickness and inner diameter measurement is highly affected by the excitation frequency and placement of the coils. In order to illustrate this dependence finite element analysis was performed.

Two cases were analysed, Fig. 1. The detector coil N_d is placed at $L=70\text{mm}$ (probe length) from the exciter coil in both cases. In the first case, Fig. 1.a, the exciter coil N_e was placed beneath the defect ($D_1=0$) and excitation frequency of 60Hz was applied. In the second case, Fig. 1.b, the exciter coil was at $D_1=L/2=35\text{mm}$ from the defect and excitation frequency of 1000Hz was used. In each case the internal and external defects were simulated. Nominal wall thickness c of 4,45mm was reduced to 3,45mm at defect location. The tube material had relative permeability $\mu_r=100$ and conductivity $\sigma=4\text{MSm}^{-1}$. Simulations were performed using FEMM freeware package [8].

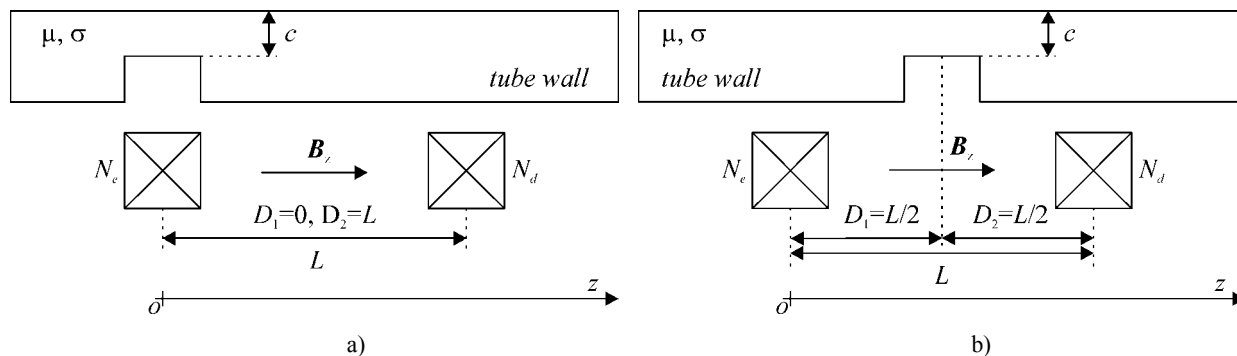


Fig. 1. Definition of axisymmetric geometry used in finite element analysis: a) the exciter coil is beneath the defect ($D_1=0$, excitation frequency 60Hz), b) defect is in the middle between the coils ($D_1=D_2=L/2$, excitation frequency 1000Hz). In both cases, the defect can be either internal or external.

2.2. Experimental set-up and procedure

Measurements were performed on two ferromagnetic steel tubes, both 1,46m long with inner diameter $R_i=51,4\text{mm}$, outer diameter $R_o=60,3\text{mm}$ and nominal wall thickness $c=4,45\text{mm}$. Three axisymmetric defects (40mm long, displaced for 320mm) with depths $d_1=1\text{mm}$, $d_2=2\text{mm}$ and $d_3=3\text{mm}$ (tolerances $\pm 0,1\text{mm}$) were machined as external on tube no. 1 and as internal on tube no. 2.

Exciter coil ($N_c=300$) and detector coil ($N_d=1100$) were fixed on a plastic rod that was inserted into the tube, axially centralized and moved along the tube as an unit. The distance between the coils was 70mm. In the conventional RFEC technique the distance is greater than 150mm.

Measurement set-up is depicted in Fig. 2. The exciter coil was fed from a power amplifier driven by a pulse generator. We applied rectangular current pulses with pulse duration of 4ms and frequency of 35Hz.

The driving current was measured with a current probe (Tektronix TM502A). Voltage induced in the detector coil was amplified using a sensitive instrumentation amplifier ($A_d=2000$, $CMRR=106\text{dB}$, $f_L=0,1\text{Hz}$, $f_H=6\text{kHz}$). Both voltages, from the current probe amplifier and the instrumentation amplifier, were digitized using 16-bit A/D converter (PC AD board HS-DAS 16) at sampling rate of 100kHz. Data processing and analysis were performed using MATLAB.

3. RESULTS

3.1. Finite Element Analysis

Amplitude and phase of the axial component of the magnetic field B_z inside the tube for geometry in Fig. 1.a (the exciter coil beneath the defect, $D_1=0$, and frequency 60Hz) are shown in Fig. 3 and Fig. 4. The results for geometry in Fig. 1.b ($D_1=35\text{mm}$ and frequency 1000Hz) are presented in Fig. 5 and Fig 6. The amplitude of magnetic field along the tube for the case without defect - B_0 , with inner defect - B_{in} , and outer defect - B_{out} , is given in Fig. 5. Ratios B_{in}/B_0 and B_{out}/B_0 are depicted in Fig. 6.

3.2. Experiments

Typical waveform of the voltage u_d induced in the detector coil is shown in Fig. 7.a. The voltage u_d can be interpreted as a superimposition of two components: a direct zone voltage u_{dz} , induced by the higher frequency components for which the detector coil is in the direct zone, and a remote zone voltage u_{rz} , induced by the lower frequency components.

Fig. 7. presents measurement results for the detector coil placed beneath the defect (distance $D_2=0\text{mm}$). Results for both, tube with external and tube with internal defects are shown in Fig. 7.a and Fig. 7.b. Relationship between zero-crossing time t_{zC} , as defined in Fig. 7.a, and the wall thickness c is depicted in Fig. 7.c.

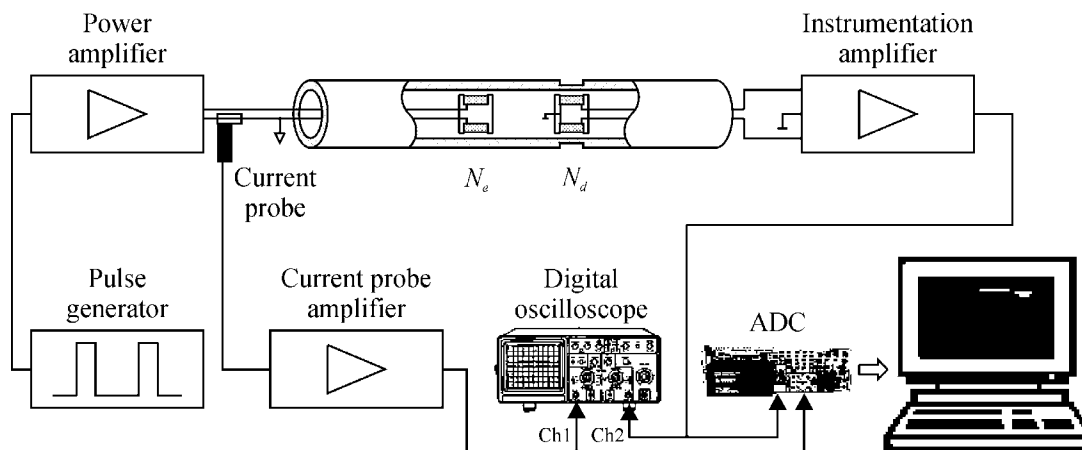


Fig. 2. Block diagram of a set-up used in measurement of the tube wall thickness and inner diameter.

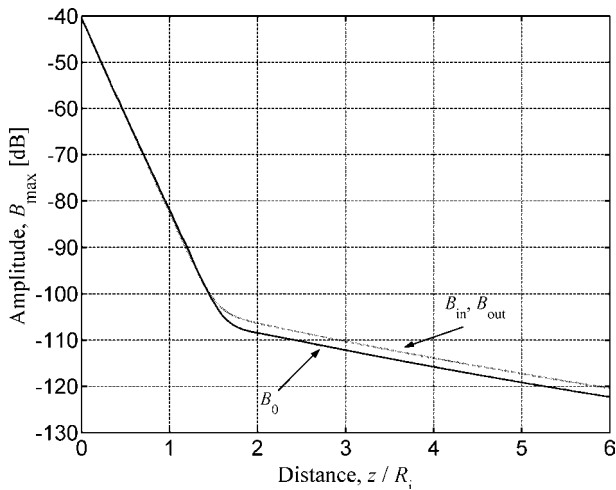


Fig. 3. Amplitude of B_z along the tube for: tube without defect – B_0 ; with inner – B_{in} ; and outer defect – B_{out} for geometry in Fig. 1.a.

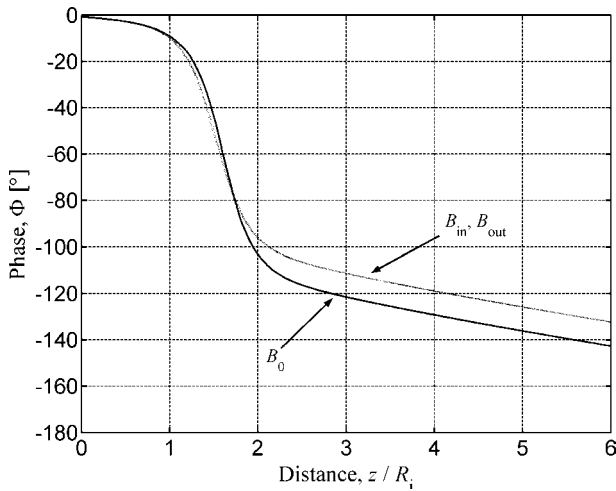


Fig. 4. Phase of B_z along the tube for: tube without defect – B_0 ; with inner – B_{in} ; and outer defect – B_{out} for geometry in Fig. 1.a.

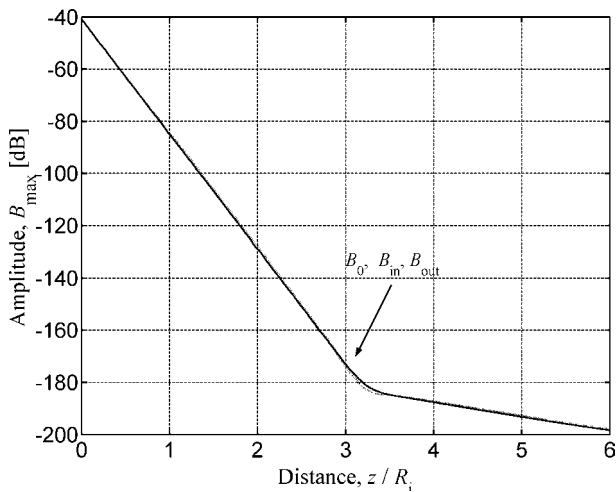


Fig. 5. Amplitude of B_z along the tube for: tube without defect – B_0 ; with inner – B_{in} ; and outer defect – B_{out} for geometry in Fig. 1.b.

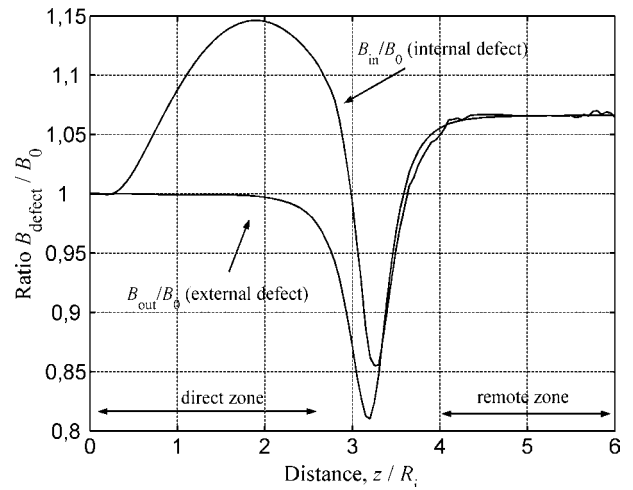


Fig. 6. Amplitude ratios B_{in}/B_0 and B_{out}/B_0 for geometry in Fig. 1.b.

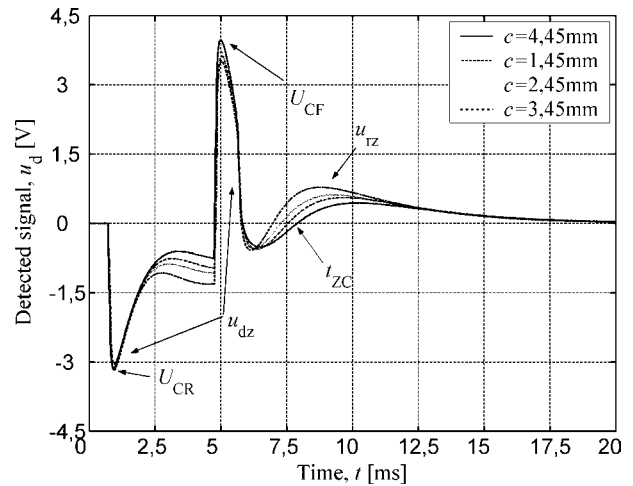


Fig. 7.a. Measurement of the wall thickness for $D_2=0$. Tube with external defects (tube no. 1).

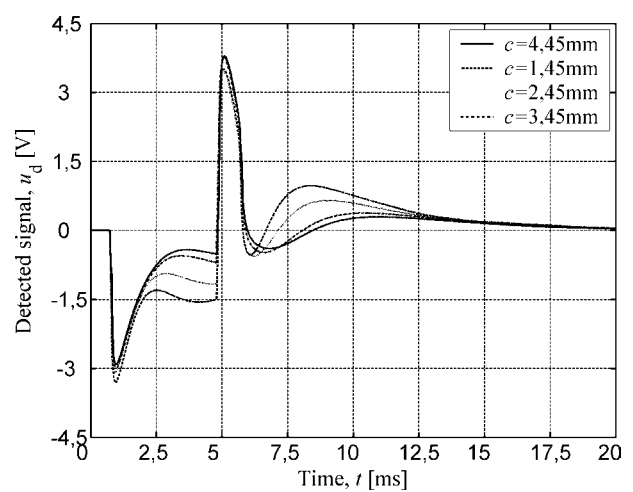


Fig. 7.b. Measurement of the wall thickness for $D_2=0$. Tube with internal defects (tube no. 2).

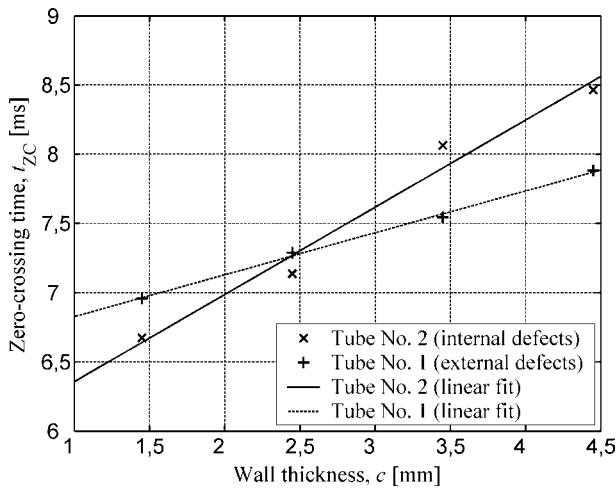


Fig. 7.c. Relationship between zero-crossing time t_{ZC} and the tube wall thickness c .

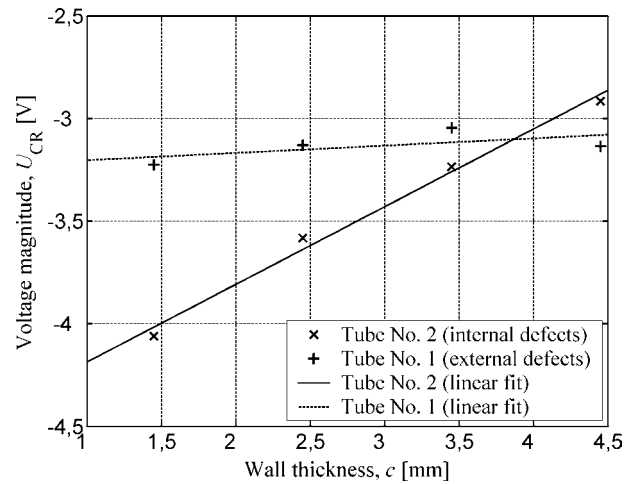


Fig. 8.c. Relationship between voltage magnitude U_{CR} and the tube wall thickness c .

Results of similar experiments, but with the defect between the coils (distance $D_1=D_2=35\text{mm}$) are given in Fig 8.a and Fig. 8.b. Relationship between voltage magnitude U_{CR} and wall thickness c is shown in Fig. 8.c.

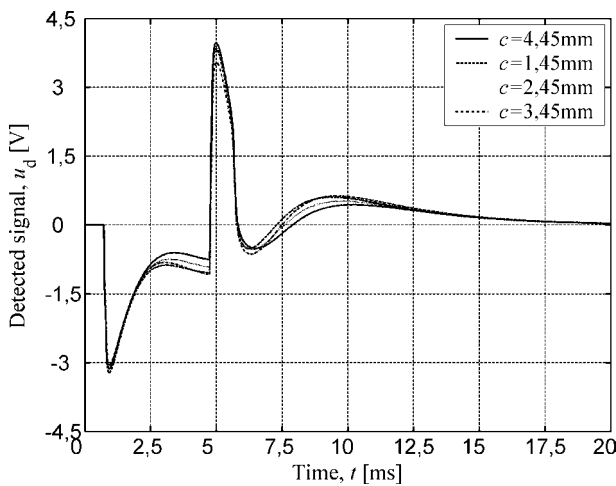


Fig. 8.a. Measurement of the inner diameter for $D_1=D_2=35\text{mm}$. Tube with external defects (tube no. 1).

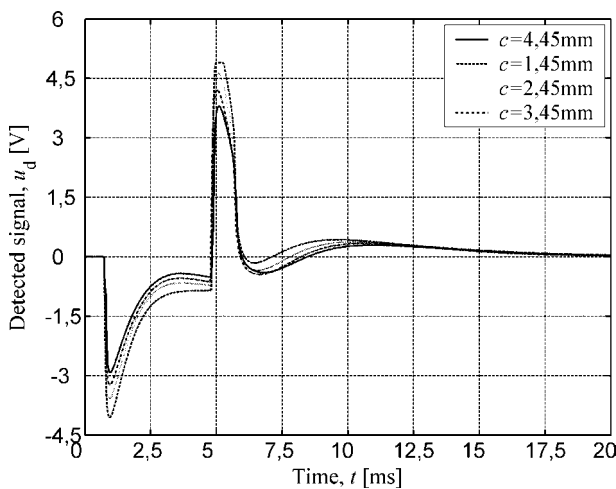


Fig. 8.b. Measurement of the inner diameter for $D_1=D_2=35\text{mm}$. Tube with internal defects (tube no. 2).

Typical log of the inner defect detection is given in Fig. 9. The zero-crossing time t_{ZC} and the voltage magnitude U_{CR} measured with spatial resolution of 10mm along the tube around the severest internal defect (wall thickness $c=1,45\text{mm}$) are recorded in a single run.

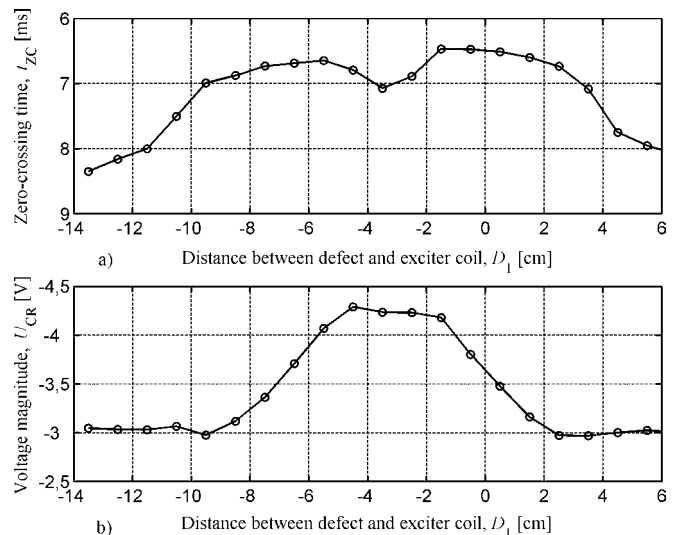


Fig. 9. Zero-crossing time t_{ZC} a), and voltage magnitude U_{CR} b), of voltage measured during the passing of the probe beneath the internal defect ($c=1,45\text{mm}$).

4. DISCUSSION

Fig. 3 and Fig. 4 (the exciter coil is beneath the defect, $D_1=0$) show an example of thickness measurement. The distance between the coils must be at least 2 inner diameters (ID) and lower excitation frequency must be applied in order to make the change of the phase or amplitude of the magnetic field measurable. However, the distinction between internal and external defect does not exist.

Fig. 5 and Fig. 6 (distance between the defect and the exciter coil is $D_1=35\text{mm}$) show an example of inner diameter measurement. According to Fig. 6, there is no difference between the magnetic field amplitudes B_{out} and B_0 in the direct zone, while significant increase of ratio B_{in}/B_0

can be observed for the internal defect. Maximal sensitivity to the inner diameter is observed for the detector coil at approximately the same distance from defect as the exciter coil (i.e. $D_1=D_2$). Closely spaced coils and high excitation frequency are *sine qua non*s of the inner diameter measurement (electrical caliper).

Experimental results for pulsed excitation, presented in Fig. 7, show that zero-crossing time t_{zC} (which is a feature of the remote zone voltage u_{tz}) is linearly related to the tube wall thickness. Different sensitivity of the measurement for tube no. 1 and no. 2, Fig. 7.c, is due to different electromagnetic properties of the tube materials.

Fig. 8 suggests how magnitude U_{CR} of the direct zone voltage u_{dz} can be used for measurement of the tube inner diameter. For the tube with the external defects (no. 1), Fig. 8.a, the change of U_{CR} with the wall thickness is negligible comparing to the case of the tube with the internal defects (no. 2), Fig. 8.b. The magnitude U_{CR} is linearly related to the change of the inner diameter caused by reduction of the wall thickness, Fig. 8.c.

Comparing Fig. 7.b and Fig. 8.b (tube no. 2) one can easily find that the greatest sensitivity to the wall thickness is obtained for the detector coil beneath the defect ($D_2=0$). The equivalent sensitivity is found when the exciter coil is at the same position ($D_1=0$), Fig. 9.a [3]. As mentioned before, sensitivity to the inner diameter is the highest when the defect is between the coils. In other words, when the probe is at a certain location, one can measure the tube wall thickness above the detector coil and, at same time, the inner diameter above the point at half the distance between the coils. The probe should be short enough to enable the observation of both voltage components.

The decrease of t_{zC} in Fig. 9.a is caused by the reduction of the tube wall thickness, while the increase of U_{CR} in Fig. 9.b indicates that this reduction is from the inside (i.e. inner defect). The existence of the first and second bump of t_{zC} is due to the passage of the detector (first) and the exciter coil (second) under the defect.

5. CONCLUSIONS

With the results of the finite element analysis we have illustrated the basic principle of the remote field technique used for wall thickness measurement and its inability to distinguish the internal and external defects. In order to measure the inner diameter, another probe with small distance between the coils and high excitation frequency is required.

We have established a methodology for measurement of both the tube wall thickness and the inner diameter with only one pair of coils. This is achieved with application of considerably shorter probe and pulsed excitation, which allows separate observation of voltage components induced by the lower and higher frequency components.

This modification results in acquisition of one excitation and one detector signal, allowing significant simplification of measurement, probe construction and electronic transducer design.

REFERENCES

- [1] J. Blitz, "Electrical and magnetic methods of non-destructive testing", Chapman & Hall, London, 1997.
- [2] D. Vasić, V. Bilas, D. Ambruš, "Pulsed Eddy Current Nondestructive Testing of Ferromagnetic Tubes", *IEEE Instrum. Meas. Technol. Conf.*, Vail, CO, USA, May 2003. In press.
- [3] T. R. Schmidt, "The remote field eddy current inspection technique", *Materials Evaluation*, vol. 42, pp. 225-230, February 1984.
- [4] I. J. McCullough, S. G. Stroud, US Patent No. 3,417,325, "Inside pipe diameter caliper using coaxial excitation and pickup coils", December 17th, 1968.
- [5] J. Yin, J. P. de Gyves, M. Lu, "In-Place Detection of Internal and External Corrosion for Underground Casing Pipes", *IEEE Int. Conf. on Industrial Technology*, China, pp. 789-793, 1994.
- [6] Y. Sun, W. C. Loo, D. C. Kunerth, T. K. O'Brien, "Finite element simulation of pulsed remote field eddy current phenomenon", *Review of Progress in Quantitative Nondestructive Evaluation*, vol.17, pp. 259-266, 1998.
- [7] D. Vasić, V. Bilas, D. Ambruš, "Measurement of ferromagnetic tube wall thickness using pulsed remote field technique", *12th IMEKO TC4 International Symposium*, Zagreb, Croatia, pp. 468-472, 2002.
- [8] Finite Element Method Magnetics (FEMM), version 3.1, January 2002, femm.berlios.de.

ACKNOWLEDGMENTS

This research has been supported by the Ministry of Science and Technology of the Republic of Croatia, grant no. 0036007 and Hotwell, Austria.

Authors:

Darko Vasić, Department of Electronic Systems and Information Processing, Faculty of Electrical Engineering and Computing, University of Zagreb, Unska 3, HR-10000 Zagreb, Croatia, Tel: (+385 1) 612 9867, Fax: (+385 1) 612 9652, E-mail: darko.vasic@fer.hr

Vedran Bilas, Department of Electronic Systems and Information Processing, Faculty of Electrical Engineering and Computing, University of Zagreb, Unska 3, HR-10000 Zagreb, Croatia, Tel: (+385 1) 612 9974, Fax: (+385 1) 612 9652, E-mail: vedran.bilas@fer.hr

Davorin Ambruš, Brodarski Institute, Av. Većeslava Holjevca 20, HR-10020 Zagreb, Croatia, Tel: (+385 1) 650 4328, E-mail: dambro@hrbi.hr